Hydrogen from ethanol reforming with aqueous fraction of pine pyrolysis oil with and without chemical looping

R. Md Zin, A.B. Ross, J.M. Jones, V. Dupont *

Energy Research Institute, School of Chemical and Process Engineering, The University of Leeds, Leeds LS2 9JT, UK

HIGHLIGHTS

- H$_2$ yield 78% of equilibrium from mix of EtOH and aqueous fraction of bio-oil at 600 °C.
- H$_2$ yield only sensitive to elemental and not chemical composition of feedstock.
- Autoreduction of Ni/alumina catalyst seen in chemical looping (CL) steam reforming.
- Low surface area Ni/α-alumina catalyst well suited to CLSR of EtOH/AQ mixture.
- High surface area Ni/γ-alumina catalyst less active due to incomplete reduction.

ARTICLE INFO

ABSTRACT

Reforming ethanol ('EtOH') into hydrogen rich syngas using the aqueous fraction from pine bio-oil ('AQ') as a combined source of steam and supplementary organic feed was tested in packed bed with Ni-catalysts 'A' (18 wt%/α-Al$_2$O$_3$) and 'B' (25 wt%/γ-Al$_2$O$_3$). The catalysts were initially pre-reduced by H$_2$, but this was followed by a few cycles of chemical looping steam reforming, where the catalysts were in turn oxidised in air and auto-reduced by the EtOH/AQ mixture. At 600 °C, EtOH/AQ reformed similarly to ethanol for molar steam to carbon ratios (S/C) between 2 and 5 on the H$_2$-reduced catalysts. At S/C of 3.3, 90% of the carbon feed converted on catalyst A to CO$_2$ (58%), CO (30%) and CH$_4$ (2.7%), with 17 wt% H$_2$ yield based on dry organic feedstock, equivalent to 78% of the equilibrium value. Catalyst A maintained these outputs for four cycles while B underperformed due to partial reduction.

1. Introduction

1.1. Aqueous fractions from bio-oils produced by fast pyrolysis and liquefaction

Solid biomasses naturally contain variable levels of moisture, which reduce their grindability and thus the efficiency of their conversion through thermochemical processes. They also have high minerals and metals content, causing emission of pollutants and corrosion during combustion. Different degrees of pre-treatments can be applied to produce clean fuels or chemical feedstocks from solid biomasses of diverse origins. The fast pyrolysis process, which utilises moderate temperatures of around 500 °C and vapour residence times below 2 s, is suitable for minimally pre-treated moist biomass, and is tolerant of a variety of feedstock. It generates volatiles with yields in the region of 70 wt%, alongside solid residues (mainly char), as well as flammable gases. Char and/or gases can be burned to sustain the process energy requirements (Bridgwater et al., 1999). After cooling, the volatiles condense into bio-oil, which, with an energy density (MJ/m^3) several times that of the original biomass, is more easily transported and stored, as well as being compatible with catalytic post-processing due to its low boiling point. However bio-oils produced in this way are rarely engine- or boiler-ready owing to high content in water (15–30 wt%) and oxygenates, placing their gross calorific value in the 16–19 MJ/kg range, i.e. roughly half that of standard, non-oxygenated, liquid fuels (Czernik and Bridgwater, 2004). Despite being considered a lower quality by-product, the water soluble fraction obtained from the liquefaction of varied types of biomass (Mosteiro-Romero et al., 2014; Neveux et al., 2014; Ye et al., 2014) is also water rich and usually represents liquefaction's highest yield on a mass basis. The compositions of bio-oil and of water soluble product of liquefaction are representative of the biomass of origin. Carbohydrates derive from the cellulose and hemicellulose biomass content, and aromatics from the lignin. The carbon- and

hydrogen-rich lignin derived compounds can be phase-separated by further adding water to the bio-oil. The lignin – also called 'organic' – fraction thus obtained can be used as a natural substitute in phenolic derived resin or may be reformulated for gasoline blending compounds. The aqueous fraction, which contains carbohydrate derived compounds and residual aromatics, has few industrial applications as food flavouring, or de-icing agent (Czernik and Bridgwater, 2004) and would pose disposal challenges as an untreated water stream. More means of recycling the aqueous fraction are sought, which would categorise it as resource rather than waste.

It has been proposed that aqueous fractions from bio-oil or liquefaction processes can be upgraded via biological means (Li et al., 2013; Sukhbaatar et al., 2014) or a reforming process which uses their water content as reagent (Kechagiopoulos et al., 2009, 2006; Medrano et al., 2011). Hydrogen is at present a valuable chemical that will be required in ever increasing amounts mainly due to population increase (38% between 2010 and 2050). This increase is mirrored in the production of ammonia-based fertilisers (Dawson and Hilton, 2011). It is also reflected in petroleum refinery operations where modern on-site steam methane reforming plants are expected to play a growing role (Harrison and Marquez, 2012). In refineries, hydrogen is increasingly outsourced, i.e. produced elsewhere and imported to the refinery (Angel, 2011). Hydrogen is gradually more utilised in hydrodeoxygenation (HDO) operations during the upgrading of biocrudes (Saidi et al., 2014). Hydrogen is also widely expected to enable the worldwide transition to a hydrogen economy, in which transportation and power generation currently relying on fossil fuels will switch to cleaner and more energy efficient hydrogen-run fuel cells (Cipriani et al., 2014).

1.2. Steam reforming of aqueous fractions of bio-oil

In the review by (Ni et al., 2007), nickel and cobalt catalysts feature prominently as active catalysts of ethanol steam reforming. Cobalt catalysts are shown to achieve ethanol conversions of 100% at temperatures as low as 623 K. However, this is achieved at very high molar steam to carbon ratios (13:1), whereas at moderate steam to carbon ratios (e.g. 3:1), only the Ni based catalysts show ability to achieve both high feedstock conversion and selectivity to hydrogen (>90%), typically for temperatures above 650 °C. When reforming aqueous bio-fractions, two major problems have been reported: (i) clogging of the feeding line due to vaporisation and (ii) coking in reactors from carbon deposits. Incorporating a cooling jacket around the feeding line can help prevent vaporization (Kechagiopoulos et al., 2006; Medrano et al., 2011), while the usual approach to prevent coking is to increase reforming temperatures in order to favour carbon steam gasification and the reverse Boudouard reaction. For instance, (Czernik et al., 2002) employed 850 °C with molar steam to carbon (S/C) ratio of 7 when steam reforming the aqueous fraction of pine sawdust bio-oil in a fluidized bed reactor. (Medrano et al., 2011) used aqueous fraction of pine bio-oil at 650 °C and S/C of 7.64, where little amounts of oxygen were introduced to gasify the coke, which eventually reduced coke deposits by 50%. The uses of elevated temperatures (>650 °C) but in particular S/C in excess of 4, can represent prohibitive energy penalties. This is illustrated for ethanol feedstock in Table 1, which compares enthalpy changes of producing 1 mol of H_2 via thermal water splitting ('WSP') with steam reforming of ethanol ('SRE') for S/C between 1 (lack of H_2O) and 12 (large H_2O excess). The calculations assumed atmospheric pressure, reactants initially in liquid phase at 25 °C and products at 650 °C, using equilibrium data generated with the CEA code (see Section 2.2.2). The heat demand of producing 1 mol of H_2 via SRE at 650 °C increases linearly with S/C in the range studied, and is dominated by raising steam at 650 °C from liquid water at ambient conditions. The heat demand of SRE becomes equal to that of thermal WSP at approximately S/C of 6.4, invalidating the need for ethanol feedstock. Table 1 also lists for S/C of 3 the ratio of total heat demand of SRE to that of thermal WSP for temperatures between 500 and 800 °C, and shows that the minimum ratio of 0.67 is reached between 600 and 650 °C, indicating SRE is at its most advantageous compared to thermal WSP.

The present study is motivated by demonstrating the conversion of aqueous fractions of bio-oils to hydrogen by steam reforming at moderate temperature (600 °C) and steam to carbon ratios below 4 without oxygen addition. The medium temperature minimises reverse water gas shift and thus favours a H_2 rich syngas. However, using lower steam to carbon ratios than those reported in the literature for bio-oil reforming are expected to lower both the maximum achievable hydrogen yield and hydrogen purity in the syngas, but should increase the thermal efficiency of the process (Table 1). Given that the aqueous fractions of bio-oils have an organic content of a few weight percent, and thus exhibit S/C ratios much higher than 10, on their own, aqueous fractions of bio-oil intrinsically far exceed the target S/C range of 2–5 for thermally efficient steam reforming. Here, the hydrogen production by steam reforming is considered thermally in-efficient when it requires more energy input (based on enthalpy balance) than when the hydrogen is produced by water splitting. To address the problem of enthalpic burden of the water reactant, we chose to combine a bio-oil aqueous fraction with another dry feedstock so as to achieve a feed mixture S/C between 2 and 5. Biomass derived aqueous fractions can add a renewable contribution to

Table 1
Heat demand of steam reforming of ethanol (SRE) compared to thermal water splitting (WSP). Terms 1 and 2: heating of reactants (EtOH and H_2O) to reformer temperature, term 3: enthalpy change of isothermal SRE reaction, all values given per mol of H_2 produced at equilibrium.
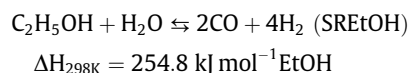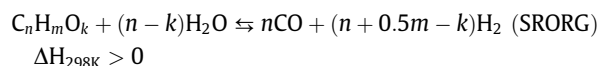
ΔH term (kJ/mol H_2) or fraction	States	Molar S/C, @ T_R = 650 °C, 1 atm						
	Initial → final	1	1.5	2	3	4	6	12
1. EtOH	298 K, liq → 923 K, vap	32.6	27.2	24.4	21.7	20.5	19.5	18.7
2. H_2O	298 K, liq → 923 K, vap	40.5	50.7	60.6	80.8	101.9	145.4	278.5
3. SRE reaction	923 K, vap → 923 K, gas	49.9	48.3	46.7	44.2	42.3	40.0	37.3
Total SRE = 1 + 2 + 3	298 K, liq → 923 K, gas	123	126	132	147	165	205	335
H_2O/total SRE	298 K, liq → 923 K, gas	0.33	0.40	0.46	0.55	0.62	0.71	0.83
WSP	298 K, liq → 923 K, gas	219	219	219	219	219	219	219
Total SRE/WSP	298 K, liq → 923 K, gas	0.56	0.58	0.60	0.67	0.75	0.94	1.53
H_2 yield (wt%)	923 K, 1 ⩽ S/C ⩽ 12	14.5	17.4	19.4	21.8	23.0	24.2	25.3
		Reformer temperature (K) @ S/C = 3, 1 atm						
		773	823	873	923	973	1023	1073
Total SRE/WSP	298 K, liq → T_R, gas	0.82	0.71	0.67	0.67	0.70	0.73	0.77
H_2 yield (wt%)	S/C = 3, 773 ⩽ T_R ⩽ 1073 K	12.4	16.6	20.0	21.8	22.1	21.9	21.6

the steam reforming of a fossil feedstock for the production of hydrogen via its use as the steam resource. It can also complement the steam reforming of a water-free biofeedstock. Due to its production routes from both fossil fuels and energy crops, its ease of transport and storage, its lack of toxicity, its high solubility in water permitting a single feed line, and its volatility, ethanol was considered a good candidate as primary dry feedstock to test its reforming with the aqueous fraction of pine pyrolysis oil instead of steam. In addition, there is extensive literature on the steam reforming of ethanol and it generates a good maximum yield of hydrogen (6 mol H_2/mol EtOH, i.e. 26.3 wt% EtOH, which exceeds the (2H) content in ethanol (13 wt%) due to the steam contribution to the H_2 produced) compared to more oxygenated biofeedstocks.
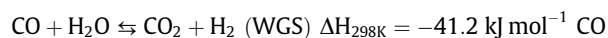
1.3. Chemical looping steam reforming of ethanol/aqueous fraction of bio-oil

A further aim of this study was to investigate the potential of chemical looping steam reforming an ethanol/bio-oil aqueous fraction feed mixture, similarly to the authors' prior findings on unseparated bio-oils (Lea-Langton et al., 2012). The latter investigation inscribed itself in a programme of research by this group on the fuel flexibility of the chemical looping steam reforming process using packed beds and alternating feed flows (as opposed to circulating bed materials under continuous feed flows), and in particular, applied to feedstock of biomass or waste origin. The chemical looping steam reforming process relies on alternating the oxidation of a catalyst under air feed with its reduction under feedstock and steam feed allowing steam reforming in near autothermal conditions (i.e. without provision of external heat, unlike the conventional process), while producing non N_2-diluted syngas, thus high H_2 content. This is despite using air for the heat-generating oxidation reactions, rather than the pure O_2 from a costly air separation unit, as do the conventional partial oxidation or conventional autothermal reforming processes.

Reforming of the organic content of the aqueous fraction and ethanol mixture using the steam from the aqueous fraction takes place according to the following stoichiometric global reactions, here termed 'SRORG', 'SREtOH', and to the water gas shift reaction 'WGS'. These are listed below for an organic feedstock of generic molar formula $C_nH_mO_k$ and for ethanol:
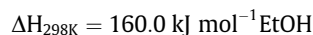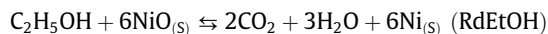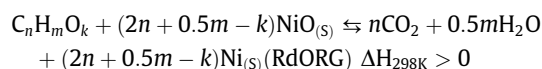
$$C_nH_mO_k + (n - k)H_2O \leftrightarrows nCO + (n + 0.5m - k)H_2 \text{ (SRORG)}$$
$$\Delta H_{298K} > 0$$

$$C_2H_5OH + H_2O \leftrightarrows 2CO + 4H_2 \text{ (SREtOH)}$$
$$\Delta H_{298K} = 254.8 \text{ kJ mol}^{-1} \text{EtOH}$$

The intermediate product CO subsequently converts to CO_2 via the water gas shift reaction ('WGS'). The conversion is incomplete due to the mild exothermicity of WGS and the higher temperatures used for steam reforming.

$$CO + H_2O \leftrightarrows CO_2 + H_2 \text{ (WGS) } \Delta H_{298K} = -41.2 \text{ kJ mol}^{-1} \text{ CO}$$
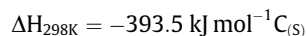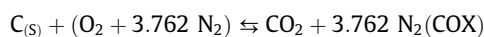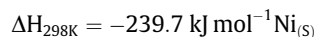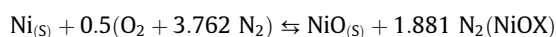
The stoichiometric molar S/C ratio of the coupled SREtOH-WGS reactions is 1.5 for complete conversion to H_2 and CO_2.

Steam reforming with chemical looping in packed bed configuration using nickel as oxygen transfer material, as well as steam reforming catalyst, is characterised by the following main reduction reactions of NiO ('RdORG', 'RdEtOH') that take place during a half cycle of the EtOH/AQ feed:

$$C_nH_mO_k + (2n + 0.5m - k)NiO_{(S)} \leftrightarrows nCO_2 + 0.5mH_2O$$
$$+ (2n + 0.5m - k)Ni_{(S)} \text{(RdORG) } \Delta H_{298K} > 0$$

$$C_2H_5OH + 6NiO_{(S)} \leftrightarrows 2CO_2 + 3H_2O + 6Ni_{(S)} \text{ (RdEtOH)}$$
$$\Delta H_{298K} = 160.0 \text{ kJ mol}^{-1} \text{EtOH}$$

Once the Ni-based OTM is reduced, SRORG, SREtOH and WGS can proceed. Supporting evidence and mechanistic information for RdORG can be found in (Cheng and Dupont, 2013) using acetic acid as the feedstock on one of the catalysts used here (catalyst 'A'). Acetic acid is a major component of not just our aqueous fraction of pine bio-oil, but also of biomass pyrolysis oils in general. In addition, side reactions such as pyrolysis, cracking, and CO disproportionation (Boudouard reaction) may result in carbon deposition during the EtOH/AQ feed half cycle. The chemical 'loop' is then completed by discontinuing the EtOH/AQ feed and starting the air feed for the second half of the cycle, which causes both the nickel and carbon oxidation reactions ('NiOX' and 'COX'):

$$Ni_{(S)} + 0.5(O_2 + 3.762 \text{ N}_2) \leftrightarrows NiO_{(S)} + 1.881 \text{ N}_2 (NiOX)$$
$$\Delta H_{298K} = -239.7 \text{ kJ mol}^{-1} Ni_{(S)}$$

$$C_{(S)} + (O_2 + 3.762 \text{ N}_2) \leftrightarrows CO_2 + 3.762 \text{ N}_2 (COX)$$
$$\Delta H_{298K} = -393.5 \text{ kJ mol}^{-1} C_{(S)}$$

2. Methods

The experimental set-up is shown in Fig. 1. The feeding system, reactor, gas and condensates collection and analysis, temperature and flow measurement have been described elsewhere and were used previously to investigate the performance of pyrolysis oils from palm empty fruit bunch (PEFB) and pine wood by chemical looping steam reforming (Lea-Langton et al., 2012) and sorption enhanced steam reforming (Md Zin et al., 2012) in packed bed reactor configuration. The aqueous fraction from pine oil was selected over that of PEFB oil in the present study due to the high lignin content in pine, which in theory makes it more suitable for upgrading for the resin industry, leaving its aqueous fraction as by-product.

2.1. Materials and characterisation

Ethanol (C_2H_5OH, density 789 kg m^{-3}) with purity $\geqslant$99.5% was purchased from Sigma–Aldrich for steam reforming with the aqueous fraction.

2.1.1. Aqueous fraction characterisation

The pine bio-oil source was purchased from Biomass Technology Group (BTG). The aqueous fraction used in this study was prepared by the water fractionation scheme (Sipila et al., 1998). This consisted in adding water into the bio-oil. The bio-oil to water mass ratio of 1:10 was selected to achieve near complete extraction of the water-soluble compounds into the aqueous fraction. The 1:10 mass ratio dilution resulted in a small amount of powdery residue sticking to the dilution vessel walls, and an aqueous fraction with a light brownish colour and fairly smoky odour. Given the negligible amounts of separation achieved with this dilution ratio, the water content of our aqueous fraction was determined by water balance. The water balance specifies that the mass of water added to the water originally present in the oil, i.e. 22 wt% (Md Zin et al., 2012) equals that of the water present in the aqueous fraction, assuming that the small amount of powdery residue was dry. Using this method, the water balance yielded 92.9 wt% water in the aqueous fraction, the remainder 7.1 wt% representing its organic content. In our earlier study, which describes the methodology for the oils characterisation (Md Zin et al., 2012), GC–MS of the original bio-oil allowed the identification of 92 organics that
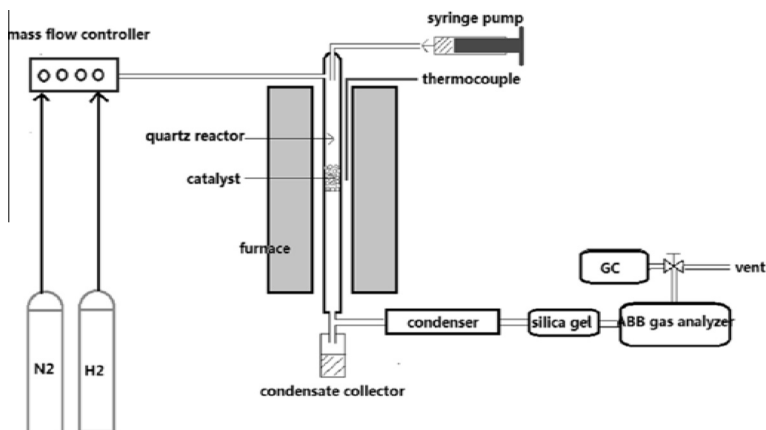
Fig. 1. Experimental set up.

accounted for 100% of the surface area of all the peaks produced. Main water soluble components were levoglucosan, acetic acid, guaiacol, 2(5H)-furanone and vanillin. Here, the molar elemental make-up of the aqueous fraction's organic content was approximated to that of the original bio-oil's: $C_{0.3372}H_{0.444}O_{0.2172}$, due to the negligible separation observed after water addition. As an example of the different compositions tested in the results section, a mixture of 3 mol of acetic acid, 1 mol of levoglucosan and 6 mol of 2(5H)-furanone yielded the molar formula of $C_{0.34286}H_{0.43810}O_{0.21905}$, which placed it within −2%, +1% and −1% of the target C, H, and O of the original bio-oil respectively (see 'M4' in Table 2). Neglecting nitrogen content, the reactions of NiO auto-reduction by the organic residue in the aqueous phase 'RdORG' and the steam reforming of the same 'SRORG' would become, specifically for this example:
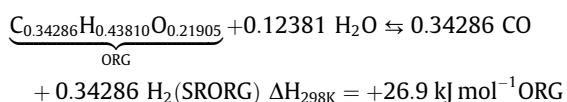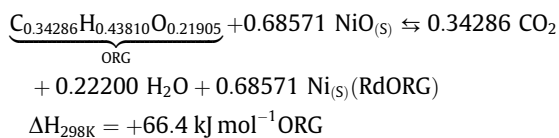
$$\underbrace{C_{0.34286}H_{0.43810}O_{0.21905}}_{ORG} +0.68571\ NiO_{(S)} \leftrightharpoons 0.34286\ CO_2$$

$$+\ 0.22200\ H_2O + 0.68571\ Ni_{(S)}(RdORG)$$

$$\Delta H_{298K} = +66.4\ kJ\ mol^{-1}ORG$$

$$\underbrace{C_{0.34286}H_{0.43810}O_{0.21905}}_{ORG} +0.12381\ H_2O \leftrightharpoons 0.34286\ CO$$

$$+\ 0.34286\ H_2(SRORG)\ \Delta H_{298K} = +26.9\ kJ\ mol^{-1}ORG$$

The 'dry' and 'wet' molar compositions for AQ were used to determine the flow rates of AQ to achieve a given molar steam to carbon ratio (S/C) when in mixture with ethanol, while the assumed individual components' mole fractions were necessary inputs to the chemical equilibrium calculations (Section 2.2.2).

2.1.2. Catalysts

Two types of catalyst were supplied in pellet form by Johnson Matthey Plc. Catalyst 'A' consisted of, when fully oxidised, ~18 wt% NiO on α-Al₂O₃ support, and catalyst B contained ~25 wt% NiO on γ-Al₂O₃ support (the latter also had small concentrations of other dopants). Catalyst A was measured for BET surface area before and after steam reforming experiment using a Quantachrome Instrument Nova 2200 and the multipoint BET (6 points) method. Due to the mesoporosity of catalyst B, the surface area and pore size for the fresh and used catalyst B were obtained using N₂ adsorption/desorption isotherm and reported using BJH method. The BET surface areas of fresh catalysts A and B were 3.3 m²/g and 50.5 m²/g respectively. Characterisation of the fresh catalyst A by XRD, SEM and TEM is described in (Md Zin et al., 2012).

2.2. Methodology

2.2.1. Experimental

The ethanol/aqueous fraction of pine bio-oil mixture ('EtOH/ AQ') was prepared prior to experimental runs according to the

Table 2
Chemical equilibrium outputs at 650 °C, 1 atm, for four different assumed aqueous fraction composition (dry basis) with target $C_nH_mO_k$ of $C_{0.3372}H_{0.444}O_{0.2172}$ of original bio-oil.

Mole fraction					Formula ORG			Molar	H_2	$X_{H2O,eq}$	Sel_{H^-}	Sel_{C^-}	Sel_{C^-}
Mix	Acetic acid	Levo-glucosan	Vanillin	2(5H) furanone	$(C_nH_mO_k)$			S/C	Yield	Conv.	H_2	CO	CH_4
	$(C_2H_4O_2)$	$(C_6H_{10}O_5)$	$(C_8H_8O_3)$	$(C_4H_4O_2)$	n	m	k		wt%	Frac.	%	%	%
M1	0.4	0.3	0.3	0	0.329	0.461	0.211	2.14	20.6	0.471	97.9	42.8	2.4
								2.57	21.2	0.419	98.8	37.4	1.4
								3.30	21.7	0.351	99.4	30.2	0.6
								4.14	21.9	0.294	99.7	24.4	0.3
M2	0.63	0.12	0.25	0	0.323	0.465	0.212	2.14	20.6	0.470	97.9	42.8	2.4
								2.57	21.2	0.418	98.8	37.3	1.4
								3.31	21.7	0.350	99.5	30.2	0.6
								4.15	21.9	0.293	99.7	24.3	0.3
M3	0	0.65	0.35	0	0.330	0.458	0.212	2.14	20.6	0.471	97.9	42.8	2.4
								2.57	21.2	0.419	98.8	37.4	1.4
								3.30	21.7	0.351	99.4	30.2	0.6
								4.14	21.9	0.294	99.7	24.4	0.3
M4	0.3	0.1	0	0.6	0.343	0.438	0.219	2.13	20.5	0.472	97.9	42.8	2.4
								2.57	21.1	0.420	98.8	37.3	1.4
								3.29	21.7	0.352	99.5	30.2	0.6
								4.13	21.8	0.295	99.7	24.3	0.3

target range of molar steam to carbon ratio ('S/C') between 2 and 5. The mixture was delivered into the reactor by a programmable syringe pump (New Era Pump Systems). The steam reforming experiments were performed at atmospheric pressure and temperature of 600 °C in the down-flow packed bed reactor system as described in (Md Zin et al., 2012), albeit with the difference that a single feed was used here as opposed to separate bio-oil/water feeds of the previous study, due to the high miscibility of alcohol in the bio-oil aqueous fraction. This temperature was within the temperature range for maximum hydrogen yield for ethanol steam reforming at S/C = 3 as predicted by chemical equilibrium calculations using the CEA code (McBride and Gordon, 1996). The experimental runs were divided into 3 stages:

(a) Steam reforming of ethanol using catalyst A for S/C = 2–5, and catalyst B at S/C = 2.
(b) Steam reforming of EtOH/AQ using A, then using B for S/C = 2.05–4.18.
(c) Chemical looping steam reforming of EtOH/AQ using A, then B for S/C = 3.33.

The pellets of A and B were crushed to 0.85–2 mm size particles and the same amount of 6 g was used for all the experimental runs. The experiment started with a 'conventional' catalyst reduction step using 5 vol% H_2/N_2 at flow rate of 320 cm^3 min^{-1} (STP). At this stage all the NiO was converted to the catalytically active phase Ni. The reduction step reached completion when the H_2 value indicated 5 vol% again at the H_2 gas analyser. The flow of H_2/N_2 mixture was then stopped and H_2 in the system was flushed using a N_2 flow of 200 cm^3 min^{-1} (STP) until the H_2 concentration subsided to zero. Following this step, the syringe pump for the mixture was switched on to start the steam reforming step.

The weight hourly space velocities (WHSV, defined by total mass flow rates of reactants including N_2 divided by mass of catalyst) were in the range 2.41–2.94 h^{-1}, calculated based on flow feeds in the ranges of 185–200 cm^3 min^{-1} (STP) of N_2, 0.46–0.9 ml/h of liquid ethanol, and 1.2–1.54 ml/h of liquid AQ, with the ethanol and AQ mixture delivered in mixture by a single syringe pump, both at ambient temperature of 22 °C and using 6 g of catalyst. Individual flow conditions are shown in the results section. Nitrogen gas was deliberately used as an inert diluent in our experiments in order to derive from a nitrogen balance the total dry molar flow of outgoing gases. This allowed performing the calculations of product yields from measurement of their dry mole fractions, as well as the conversions of fuel (combined ethanol and organic content in aqueous fraction) and of steam from the aqueous fraction. In a 'real world' process, the addition of an inert diluent like nitrogen would neither be necessary nor recommended except for purging purposes as it would, amongst other effects, decrease the purity and calorific value of the reformate.

After completing the steam reforming phase, N_2 was kept flowing until the concentrations of outgoing gases had subsided to zero, then the N_2 feed was stopped.

The oxidation step of the chemical looping reforming experiments took place at a set temperature 600 °C using an air flow of 970 cm^3 min^{-1} (STP). The oxidation reactions gave rise to an increase in reactor temperature. This ended when the temperature in the reactor returned back to the initial 600 °C, indicating combustion of carbon deposits on the nickel catalyst and re-oxidation of the nickel catalyst were no longer taking place.

For the experiment using catalyst A, the temperature for reduction, steam reforming and oxidation steps were at 600 °C. Catalyst B was reduced by H_2 at 500 °C but underwent steam reforming and oxidation steps at 600 °C.

2.2.2. Chemical equilibrium calculations

The code Chemical Equilibrium and Applications 'CEA' (McBride and Gordon, 1996) was used to calculate equilibrium conditions of the EtOH/AQ system at atmospheric pressure and temperatures corresponding to the experiments. This code relies on minimisation of Gibbs free energy and therefore requires as set of input data comprising the thermodynamic properties enthalpy, entropy and specific heat, and their variations with temperature for the pool of reactants and products, in addition to pressure, temperature and molar inputs (initial conditions). The code allows taking into account the full population of chemical species in the code's library (thermo.inp) as potential equilibrium products, which includes hundreds of stable hydrocarbon species and free radicals, as well as ions, in gaseous and condensed phases. However, the standard version of thermo.inp does not include thermodynamic properties of unusual species that are nevertheless typical of bio-oils, therefore these were found in other sources and incorporated in the program. Accordingly, the thermodynamic properties of acetic acid ($C_2H_4O_2$) were from (McBride and Gordon, 1996) and were present in the original thermo.inp file, but those of levoglucosan ($C_6H_{10}O_5$) and 2(5H)-furanone were taken from (Catoire et al., 2008), whereas vanillin's ($C_8H_8O_3$) were from (Yaws, 2009).

2.2.3. Methodology of outputs calculations

The outputs of the equilibrium calculations (subscript 'eq') and of the experimental runs ('exp') are presented using the following equations which permit their comparison with each other. In the equations, the symbol n_i represents the molar amount for the equilibrium calculations, and $\dot{n}_i$ the molar flow rate in the experimental runs. The feedstock 'fuel' (ethanol, or combined ethanol with organic content of the bio-oil aqueous fraction) is represented in the equations listed below by a dry 'combined' molar formula $C_nH_mO_k$ of organic feedstock. The combined fuel's molar formula changed with S/C ratio according to the constant organic content in the aqueous phase, i.e. increasing S/C resulted in a higher fuel feed and vice versa, this is clear in the compositions listed in Table 3.

The hydrogen yield was presented on a mass basis compared to the dry combined fuel feed, where $\bar{W}$ is the relevant molar mass:

$$H_2 \text{ yield}_{,eq} \text{ (wt\%)} = 100 \times \frac{\bar{W}_{H_2} \times n_{H_2}}{\bar{W}_{fuel} \times n_{fuel}} \qquad (1.1)$$

$$H_2 \text{ yield}_{,exp} \text{ (wt\%)} = 100 \times \frac{\bar{W}_{H_2} \times \dot{n}_{H_2}}{\bar{W}_{fuel} \times \dot{n}_{fuel}} \qquad (1.2)$$

The total molar flow rate of outgoing gas $\dot{n}_{tot}$, needed to solve Eqs. (1)–(3) ($\dot{n}_i = y_i \times \dot{n}_{tot}$ for the experiments, and $n_i = y_i \times n_{tot}$ for equilibrium calculations, where y_i was the relevant mol fraction), was determined by nitrogen balance, with N_2 assumed inert in the experiments, but resulting in the aforementioned negligible amount of NH_3 at theoretical equilibrium.

Table 3
Molar inputs of chemical equilibrium calculations for EtOH/AQ mixture at varying S/C, using the dry mixture 'M1' for the organic content of the aqueous fraction, where the aqueous fraction consists of 7.1 wt% organic content (M1) and 92.9 wt% water. Total moles of input = 1000.

S/C	2.136	2.569	3.298	4.135
C_2H_6O	24.01249	20.77717	16.55743	13.26508
H_2O	117.1361	125.4856	135.088	144.4225
N_2	857.4899	852.2786	846.7843	840.6336
$C_2H_4O_2$	0.544624	0.583445	0.628082	0.671493
$C_6H_{10}O_5$	0.408468	0.437584	0.471062	0.50362
$C_8H_8O_3$	0.408468	0.437584	0.471062	0.50362

The maximum theoretical H_2 yields assuming complete conversion to H_2 and CO_2 were 26.30 wt% for ethanol alone, and 17.05 wt% for the organics in the aqueous fraction.

A hydrogen yield efficiency was then defined as:

$$\%H_2 \text{ yield eff} = 100 \times H_2 \text{ yield},_{exp}/H_2 \text{ yield},_{eq} \tag{1.3}$$

Thus a hydrogen yield efficiency close to 100% would represent a system close to equilibrium and a maximum achievable for the chosen feed and reaction conditions.

Fuel conversion to main carbon containing gases was defined from the carbon element balance:

$$X_{\text{fuel, eq}} = \frac{n_{\text{fuel,in}} - n_{\text{fuel,eq}}}{n_{\text{fuel,in}}} \tag{2.1}$$

$$X_{\text{fuel, exp}} = \frac{\dot{n}_{CO} + \dot{n}_{CO_2} + \dot{n}_{CH_4}}{n \times \dot{n}_{\text{fuel}}} \tag{2.2}$$

$X_{\text{fuel,exp}}$ differs from $X_{\text{fuel,eq}}$ in that only the three gas products CO, CO_2 and CH_4 were taken into account in the experimental fuel conversion value.

Water conversion was estimated from the above using a hydrogen element balance:

$$X_{\text{H2O,eq}} = \frac{n_{H_2O,in} - n_{H_2O,eq}}{n_{H_2O,in}} \tag{3.1}$$

$$X_{\text{H}_2\text{O,exp}} = \frac{(4\dot{n}_{CH_4} + 2\dot{n}_{H_2} - mX_{\text{fuel,exp}}\dot{n}_{\text{fuel}})}{2\dot{n}_{H_2O,in}} \tag{3.2}$$

Selectivity to carbon containing products CO, CO_2 and CH_4 were calculated using three equations, here shown for only for CO:

$$\text{Sel}_C\text{CO}_{\text{exp or eq}}(\%) = 100 \times \frac{y_{CO}}{y_{CO} + y_{CO_2} + y_{CH_4}} \tag{4}$$

$\text{Sel}_C \text{ CO}_2 \text{ }_{\text{exp or eq}}$ and $\text{Sel}_C \text{ CH}_4 \text{ }_{\text{exp or eq}}$ corresponded to Eqs. (5) and (6) respectively (not shown).

Selectivity to hydrogen containing products H_2, CH_4 and NH_3 used three equations, here shown only for H_2:

$$\text{Sel}_H\text{H}_{2\text{exp or eq}} = 100 \times \frac{y_{H_2}}{y_{H_2} + 2y_{CH_4} + 1.5y_{NH_3}} \tag{7}$$

with $\text{Sel}_H \text{ CH}_4 \text{ }_{\text{exp or eq}}$ and $\text{Sel}_H \text{ NH}_3 \text{ }_{\text{exp or eq}}$ corresponding to Eqs. (8) and (9) respectively (not shown).

For $\text{Sel}_H \text{ }_{\text{exp}}$, only the selectivity to H_2 and that to CH_4 were measured. In $\text{Sel}_H \text{ }_{\text{eq}}$, $\text{Sel}_H \text{ NH}_3$ was determined and found to be very small at 600 °C (0.05–0.06%).

During chemical looping steam reforming, the reduction of NiO reactions RdEtOH and RdORG precede the catalytic steam reforming reactions SREtOH and SRORG due to the lack of reduced, metallic nickel in the reactor bed, which is the catalytically active material for the SR and WGS reactions.

An important requirement for good operation of the chemical looping steam reforming process is that the Ni bed material is able to maintain the same extent of oxidation and reduction over repeated cycles. This was calculated via the rate of NiO reduction to Ni as follows, based on an oxygen element balance as previously used in (Pimenidou et al., 2010) for a fuel of molar formula $C_nH_mO_k$:

$$\dot{n}_{\text{NiO}\rightarrow\text{Ni},calc} = (\dot{n}_{CO} + 2\dot{n}_{CO_2} + 2\dot{n}_{O_2}) - (\dot{n}_{H_2O,in}X_{\text{H}_2\text{O,exp}}) - k(\dot{n}_{\text{fuel}}X_{\text{fuel,exp}}) \tag{10.1}$$

A reduction rate efficiency was defined, which compared with time on stream the rate of NiO → Ni obtained experimentally via oxygen balance (Eq. (10.1)) to the maximum possible theoretical rate according to the stoichiometry of the reduction reactions RdEtOH and RdORG:

Reduction rate efficiency (%)

$$= 100 \times \frac{\dot{n}_{\text{NiO}\rightarrow\text{Ni},calc}}{(2n + 0.5m - k)\dot{n}_{\text{fuel}}} \tag{10.2}$$

Finally the extent of NiO reduction was calculated using:

$$\%\text{NiO} \rightarrow \text{Ni(calc)} = \int_0^{t_{ss}} \dot{n}_{\text{NiO}\rightarrow\text{Ni}}dt \tag{11}$$

where t_{ss} was the time at which steady state gas compositions values were reached following the reduction period. A distinction is made here between calculated and measured extent of NiO reduction, as in some cases a measured value can be derived directly from powder XRD spectra using Rietveld refinement. This was done for our previous bio-oil and model compounds steam reforming experiments (Cheng and Dupont, 2013; Md Zin et al., 2012).

3. Results and discussion

Much of the discussion makes use of comparisons between experimental outputs with their chemical equilibrium counterparts. The first set of results aims to show that uncertainties regarding the composition of the aqueous fraction did not influence the chemical equilibrium outputs for the range of conditions studied. Table 2 lists the main chemical equilibrium outputs assuming four different bio-oil aqueous fraction mixtures, based on varying mole fractions of four model organic compounds identified in the GC–MS of the original oil. These were acetic acid, levoglucosan, and 2(5H)-furanone or vanillin, where all four were detected in significant amounts by the GC–MS although the method fell short of full quantification. These mixtures targeted the same elemental molar composition of the original bio-oil ($C_{0.3372}H_{0.444}O_{0.2172}$) and were well within 5% of the target for each of the C, H and O elements. They would have resulted in less than 2% discrepancy in maximum theoretical hydrogen yield compared to the original bio-oil.

The results in Table 2 show the chemical equilibrium outputs were found to be remarkably constant across all four assumed mixtures for any given (S/C) tested in the experiments, despite the water conversion and the selectivity to carbon containing gases varying significantly with changing S/C for a given mixture. In the following section, and for the sake of simplicity, the results of the reforming tests are shown for mixture composition 'M1', i.e. where the organic content of the AQ fraction consisted of 40 mol% acetic acid, 30 mol% levoglucosan and 30 mol% vanillin. Note that if this mixture had been attempted in practice, a small amount of preheating of the liquid mixture might have been required to fully dissolve the vanillin. On this basis, the molar inputs used for the chemical equilibrium calculations at the different steam to carbon ratios corresponding to the experiments are listed in Table 3, using an arbitrary total input of 1000 mol.

Values in Table 3 are presented with 6 decimals which were deemed required to achieve the target 7.1 wt% of organics in the aqueous phase, caused by the large molar mass of levoglucosan and vanillin. It also demonstrates the increase in mole fractions of the bio-oil compounds with increasing S/C, as the water input was linked with the bio-oil aqueous fraction input and therefore to its organic content.

3.1. Conventional steam reforming of EtOH, and reforming of EtOH with AQ

Conventional steam reforming of ethanol has been extensively studied in the literature and the aim for the experiments on ethanol alone of the present study was to provide a benchmark with

which to compare the EtOH/AQ experiments. Table 4 and Fig. 2 contain the results obtained using both catalysts A and B at atmospheric pressure and 600 °C with respect to the equilibrium values in the S/C range 2–5. Table 4 compiles the H_2 yields (exp. and eq.) and H_2 yield efficiency data for the steam reforming with ethanol (top part of table) and with the EtOH/AQ mixture (lower part). Fig. 2 plots reactants conversion and selectivity to carbon products.

Both catalysts fulfilled the expectation of processes dominated by SREtOH and WGS reactions, with carbon products composed of, in decreasing order, CO_2, CO and CH_4 at given S/C ratio, as expected at the medium temperature of 600 °C which still favours WGS over its reverse. The selectivity to CO_2 increased with S/C, as an effect of Le Chatelier's principle on both SREtOH and WGS.

Process outputs from catalyst A were consistent with a reactor that was close to, but not quite at equilibrium, with ethanol conversion between 0.9 and 1, and steam conversion approximately 75% of the equilibrium value for the S/C range studied, indicating the presence of rate-limiting undesirable reactions (i.e. methanation), evidenced by the higher selectivity to methane. In contrast, the experiment with catalyst B at S/C of 2 exhibited all its outputs consistent with chemical equilibrium. The findings were in agreement with (Aupretre et al., 2002), which also used Ni metal on alumina support. Ni is known for its good activity for cleavage of C–C and limited activity for WGS, so, high selectivity to CO_2 showed both catalysts and in particular B had good activity for the water gas shift.

As expected from Le Chatelier's principle, the H_2 yield increased with S/C at equilibrium and this was also the case in the

experiments. For catalyst A, the highest H_2 yield was achieved at the highest S/C tested (= 5), corresponding to the best oil conversion to the carbon products CO, CO_2 and to a much smaller extent, CH_4. It is also worth noting that $Sel_C CH_4$ $_{exp}$ decreased from 9.3% to 3.8% with S/C increasing from 2 to 5. This condition reflected the equilibrium trends which favour the steam methane reforming reaction at the expense of its reverse reaction (methanation of CO) at this temperature. H_2 yield efficiency, which compares the experimental yield with its equilibrium value, increased from 80% at S/C of 2 to 89% at S/C of 5 for catalyst A, confirming conditions not quite at equilibrium, whereas that of catalyst B at S/C was 97%, substantiating B as a more active catalyst for conventional ethanol steam reforming than A. The higher activity of B could be attributed to a surface area of an order of magnitude higher than that of A, as well as to its higher Ni content.

The lower part of Table 4 contains the H_2 yield outputs over catalysts A and B for the EtOH/AQ mixture, while Fig. 3 presents the variation with S/C of the reactants conversion fractions (2a), as well as the selectivity to CO_2, CO and CH_4 products (2b). As before, and for both catalysts, increasing S/C in the low range (2–3) had a beneficial effect on the H_2 yield and caused a shift to CO_2 as the main carbon product at the expense of both CO and CH_4, consistent with progressively more favourable conditions for SREtOH, SRORG and WGS. However, increasing S/C ratio beyond 3 resulted in slightly lower H_2 yield, a common occurrence with Ni catalysts, and attributed to adsorption of H_2O on the Ni active sites, thus inhibiting adsorption of the fuel, eventually causing less fuel conversion. (Marquevich et al., 2001) found that organic and steam

Table 4
Hydrogen yield and efficiency for S/C of 2–5, the two types of mixture feeds (ethanol/water, and ethanol/pine AQ) and both catalysts.

| S/C	Ethanol (ml/h)	Water (ml/h)	N_2 (cm^3/min)	WHSV (h^{-1})	H_2 yield exp (wt%)	H_2 yield eq (wt%)	H_2 yield eff (%)
Catalyst A							
1.98	0.9	1.1	196	2.58	16.9	21.2	79.7
3.01	0.7	1.3	196	2.59	18.8	23.0	81.8
4.07	0.57	1.43	200	2.64	18.5	24.0	77.2
4.99	0.49	1.51	200	2.65	21.6	24.3	88.7
Catalyst B							
2.05	0.75	0.85	185	2.41	20.8	21.5	97.1
Catalyst A	Ethanol	Pine AQ					
2.15	0.8	1.2	196	2.82	17.6	20.6	85.4
2.59	0.7	1.3	197	2.85	17.6	21.2	82.9
3.33	0.57	1.43	200	2.92	17.0	21.7	78.4
4.18	0.46	1.54	200	2.94	16.4	21.8	75.2
Catalyst B							
2.15	0.8	1.2	196	2.82	16.7	20.6	81.0
3.33	0.57	1.43	200	2.92	17.5	21.7	80.8
4.18	0.46	1.54	200	2.94	15.8	21.8	72.4
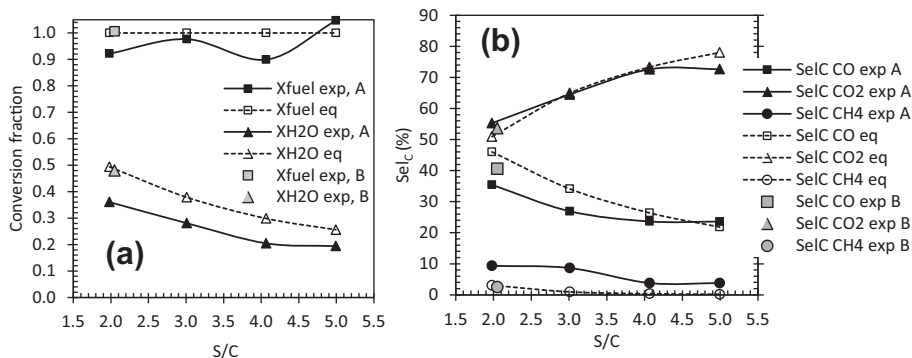
Fig. 2. Conversion of EtOH and of water during steam reforming of ethanol (a), and selectivity to carbon containing gases (b) against S/C ratio at 600 °C for the experiments (solid lines) and calculated values at chemical equilibrium (dashed lines).
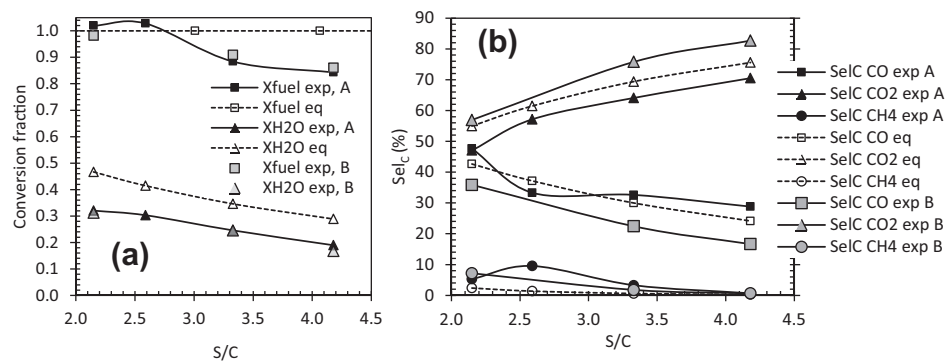
Fig. 3. Conversion of combined organic contents of EtOH/AQ, conversion of water during reforming of ethanol with aqueous fraction of pine bio-oil (a), and selectivity to carbon containing gases (b) against S/C at 600 °C for the experiments and calculated values at chemical equilibrium.

molecules competed for active sites and increasing S/C ratio caused lack of active site for the organic molecules to be adsorbed. This finding was also supported by previous studies using a Ni-based catalyst for steam reforming of acetic acid (Cheng and Dupont, 2013; Hu and Lu, 2007) and aqueous phase of rice husk at temperature 800 °C and S/C ratio of 4.9 (Yan et al., 2010). Given that acetic acid is a significant component of the aqueous fraction of our bio-oil, it was not surprising to encounter the same effect during steam reforming of EtOH/AQ on the same catalyst.

For a given S/C, the H_2 yield from EtOH/AQ for catalyst A was higher than that obtained with catalyst B, in contrast with the ethanol experiments, with A bringing conditions closer to equilibrium than B, as reflected in the H_2 yield efficiency. In addition, closeness to equilibrium was realised for the lower S/C, the root of this being evident in the drop in fuel conversion fraction from 1 to 0.85 observed when increasing S/C from to 2 to 4. The respective contents in ethanol and in bio-oil organics were such that the organics content was also increasing with S/C, as seen in Table 3. This would have caused more complex steam reforming conditions than with ethanol alone as S/C increased.

Although catalyst A showed overall better performance for catalytic reforming of the EtOH/AQ mixture, its higher selectivity to CH_4 and to CO than catalyst B is worth noting. Higher selectivity to CH_4 indicates favourable conditions for methanation of CO and CO_2, and represents a large penalty in H_2 yield, as each mole of CH_4 could have potentially steam reformed into 4 mol of H_2. High Sel_CCH_4 may also imply poor performance of a catalyst that is not able to steam reform the CH_4 produced by thermal decomposition or cracking of the fuel due to the temperature limited to 600 °C. The presence of substantial amounts of solid carbonaceous deposits that were observed at the lower, downstream, part of the reactor when reforming EtOH/AQ using catalyst A, which had persisted after a regenerative air feed step, indicated that thermal decomposition of the fuel to carbon had occurred. Coke deposition has also been reported when steam reforming aqueous fraction at temperatures between 500 and 650 °C (Li et al., 2009; Medrano et al., 2011). In contrast, and despite its slightly lower fuel conversion, reforming of EtOH/AQ using catalyst B did not result in solid deposits for this set of experiments. The higher Sel_CCO_2, $_{exp}$ for B than A also indicated catalyst B had more water gas shift activity, as found earlier for the experiments with ethanol alone.

Based on the outputs of Table 4 and Fig. 3, and mainly due to low selectivity to CH_4 and considerations of the cost of raising the AQ feed to vapour phase, which increases with S/C, the condition of S/C ratio 3.33 at 600 °C was selected for the feasibility tests of chemical looping of the EtOH/AQ mixture. In these conditions, an industrial process could feature recycle of the unconverted fuel and steam. In contrast, a high selectivity to CH_4 resulting from operating at a lower S/C would have remained problematic at the temperature of 600 °C degrees, which is, according to equilibrium predictions, insufficient for complete conversion of methane through steam reforming at atmospheric pressure.

3.2. Chemical looping steam reforming (CLSR) of EtOH-AQ

Two sets of chemical looping steam reforming were performed using the EtOH/AQ mixture with S/C 0f 3.33, using catalysts A and B. The performances of catalysts A and B as oxygen transfer catalysts in the chemical looping steam reforming process were investigated for experiments at 600 °C using 6 g of catalyst per run.

The mean process outputs at steady state during chemical looping steam reforming of ethanol with the pine bio-oil aqueous fraction are shown in Table 5 and Fig. 4 for a short number of cycles aimed at exploring feasibility of the process. The time on stream over which the mean values were calculated was around 1 h.

The steam reforming outputs after reduction of the catalyst are influenced by the reduction process that preceded it. Therefore, the calculation of the reduction rate efficiency using the EtOH/AQ mixture according to Eqs. (10.1) and (10.2) respectively was performed for the four cycles of chemical looping steam reforming. Typical plots of the reduction rate efficiency for the first 2000 s using catalysts A and B are shown in Fig. 5, while the extent of reduction by 1000 s of time on stream, where the reduction rates had fallen back to near zero for both catalysts, are listed in the last column of Table 5.

According to Table 5, the EtOH/AQ feed was able to maintain the extent of reduction of catalyst A to above 85% before the steady state of steam reforming was reached, while catalyst B achieved below 15% in the same amount of time. For catalyst A, the only gas products during the first 800 s of the reduction period were CO_2 and H_2O, reflecting that the reduction reactions RdORG and RdEtOH were not competing with the steam reforming SRORG

Table 5
H_2 yield and extent of NiO reduction to Ni (Eq. (11)) with cycle number for the two catalysts during EtOH/AQ chemical looping steam reforming at S/C of 3.33 and 600 °C.

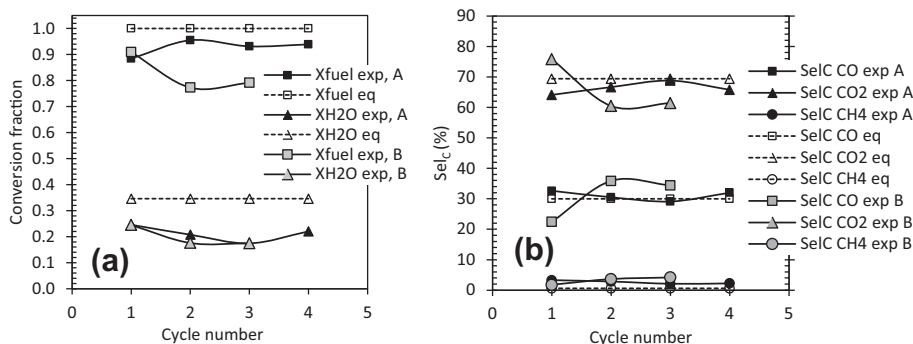| Cycle number	H_2 yield exp wt%	H_2 eff % exp/eq	%calc NiO → Ni at 1000 s
Catalyst A			
1	16.97	78.4	N/A
2	16.78	77.5	84.4
3	15.68	72.4	86.1
4	17.07	78.8	87.1
Catalyst B			
1	17.51	80.8	N/A
2	13.70	63.3	11.6
3	13.83	63.9	14.2

Fig. 4. Conversion of combined organic contents of EtOH/AQ, conversion of water during reforming of ethanol with aqueous fraction of pine bio-oil (a), and selectivity to carbon (b).
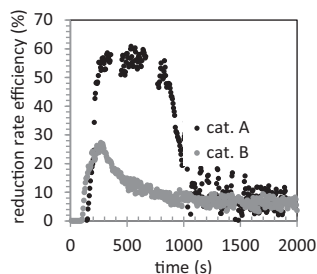

Fig. 5. Reduction rate efficiency of NiO to Ni (Eq. (10.2)) for catalysts A and B using EtOH/AQ feed (600 °C, S/C = 3.33).

Table 6
BET surface area for as received, reduced, and used catalysts.

Sample cat A	Conditions	BET ($m^2 \, g^{-1}$)
As-received	Oxide	3.262
Reduced	H_2 reduced	3.720
Used (conventional SR)	After air feed	3.547
		3.105
Used (CLR)	After air feed	2.440

and SREtOH, and bringing the extent of NiO conversion to 70%. A steady rise in CO and H_2 in the last 200 s (not shown) indicated that for the final reduction period, steam reforming was also taking place. For catalyst B, which exhibited evolution of H_2, CO, and CO_2 from the start of the experiment, the co-existence of both reduction and steam reforming mechanisms was clear, dominated by steam reforming, given the small reduction rate efficiency and nevertheless high fuel conversion. In the situation where the reduction reactions (RdORG and RdEtOH) and steam reforming co-exist, it is to be expected that the latter be affected by the equilibrium shift that the production of CO_2 and H_2O via reduction would trigger. It may therefore be desirable that reduction and steam reforming are mutually exclusive, with the reduction stage completed as quickly as possible, as observed for catalyst A. One feature that could overcome this particular drawback would be the introduction of in-situ CO_2 capture in the reformer which would introduce new favourable equilibria states for both reduction and steam reforming. We are in the process of investigating this particular effect for a future publication. The effect of chemical looping, where CLSR effectively relies on the organic content in the feed mixture to reduce the catalyst, as opposed to externally provided hydrogen (a feature we call 'auto-reduction'), can be seen in the evolution of the outputs from cycle 1 (H_2-reduced) to subsequent cycles (auto-reduced). The results in Table 4 indicate that catalysts A and B were affected very differently by reliance on auto-reduction. Catalyst A, which maintained its extent of reduction to around 78%, exhibited fuel and water conversions that retained their initial values by cycle 4, overall resulting in an unaffected H_2 yield of ca. 17 wt%, that is, 79% of the equilibrium H_2 yield. Surface areas for fresh, reduced and used catalyst A after steam reforming and chemical looping runs are listed in Table 6. Surface area of catalyst A after conventional steam reforming run followed with an air feed at set temperature of 600 °C increased very slightly from 3.3 (fresh) to 3.5 $m^2 \, g^{-1}$. In contrast, a more significant loss of surface area (down to 2.4 $m^2 \, g^{-1}$) was observed after 4 cycles via chemical looping. This was probably caused by sintering via the exotherms resulting from oxidation of Ni, and to a smaller extent, of coke under air feed. Despite this loss in surface area, the H_2 yield, as well as the fuel and water conversions, were maintained.

Catalyst B, which featured only partial reduction, exhibited a significant drop in H_2 yield from 81% to 64% in just 3 cycles, the root of which can be traced to a large slump in fuel conversion. It is proposed that this is directly related to the state of partial reduction of B throughout cycle 2, and therefore evidence of a very significant decrease in active sites for steam reforming and water gas shift compared to the fully H_2-reduced catalyst conditions of cycle 1. From cycles 2 and 3, the extent of reduction was maintained at this low level, and most of the process outputs were sustained as well, which reinforces this explanation. Concurrent with this deactivation of catalyst B due to partial reduction, the selectivity to CH_4 was found to increase steadily with cycling, as a larger proportion of the fuel would have undergone pyrolysis rather than steam reforming comparing cycle 1 with 3, accompanied by both CH_4 and coke as products.

These results therefore support the premise that for good operation of chemical looping steam reforming of EtOH/AQ, the extent of NiO reduction needs to be maintained in order to prevent catalyst deactivation and subsequent drop in conversion with build-up of undesirable by-products. It also permits the interesting conclusion that a conventionally 'better' steam reforming catalyst (as expressed by a higher surface area caused by mesoporosity, and higher number of active sites) shown to perform very well with a simple oxygenated feedstock such as ethanol, i.e. catalyst B, does not necessarily maintain high performance in chemical looping steam reforming conditions, where reducing properties under cyclic operation play such a crucial role, nor when using more complex feedstock. Here, catalyst A, which is a low surface area steam reforming catalyst, produced results exceeding expectations and outperformed catalyst B in H_2 yield, both during conventional steam reforming of the EtOH/AQ feed, as well as during its chemical looping steam reforming. Clearly, a study with a larger number of cycles on catalyst A, evaluating the energy demand of the process compared to that of the conventional process would be justified on the basis of this study.

4. Conclusion

Both catalysts A (low surface area, low Ni) and B (high area, high Ni) converted efficiently ethanol/aqueous fraction of pine pyrolysis oil mixtures. During chemical looping steam reforming experiments using A, the EtOH/AQ feed achieved close to 87% chemical reduction of NiO to Ni over cycles, maintaining a 17 wt% H_2 yield, i.e. 79% of equilibrium. A lower NiO reduction (14%) was achieved with B, resulting in a drop in H_2 yield and a growing selectivity to the undesirable product CH_4, leading to conclude that catalyst A appeared to be more suitable for CLSR of EtOH/AQ compared to B.

Acknowledgements

References

Angel, S., 2011. PRAXAIR Global Hydrogen Growth Investor Day, Global Growth Outlook.

Aupretre, F., Descorme, C., Duprez, D., 2002. Bio-ethanol catalytic steam reforming over supported metal catalysts. Catal. Commun. 3, 263–267.

Bridgwater, A.V., Meier, D., Radlein, D., 1999. An overview of fast pyrolysis of biomass. Org. Geochem. 30, 1479–1493.

Catoire, L., Yahyaoui, M., Osmont, A., Gokalp, I., 2008. Thermochemistry of compounds formed during fast pyrolysis of lignocellulosic biomass. Energy Fuels 22, 4265–4273.

Cheng, F., Dupont, V., 2013. Nickel catalyst auto-reduction during steam reforming of bio-oil model compound acetic acid. Int. J. Hydrogen Energy 38, 15160–15172.

Cipriani, G., Di Dio, V., Genduso, F., La Cascia, D., Liga, R., Miceli, R., Ricco Galluzzo, G., 2014. Perspective on hydrogen energy carrier and its automotive applications. Int. J. Hydrogen Energy 39, 8482–8494.

Czernik, S., Bridgwater, A.V., 2004. Overview of applications of biomass fast pyrolysis oil. Energy Fuels 18, 590–598.

Czernik, S., French, R., Feik, C., Chornet, E., 2002. Hydrogen by catalytic steam reforming of liquid byproducts from biomass thermoconversion processes. Ind. Eng. Chem. Res. 41, 4209–4215.

Dawson, C.J., Hilton, J., 2011. Fertiliser availability in a resource-limited world: production and recycling of nitrogen and phosphorus. Food Policy 36, S14–S22.

Harrison, S., Marquez, M., 2012. The key to the lock. Hydrocarbon Eng.

Hu, X., Lu, G., 2007. Investigation of steam reforming of acetic acid to hydrogen over Ni–Co metal catalyst. J. Mol. Catal. A Chem. 261, 43–48.

Kechagiopoulos, P.N., Voutetakis, S.S., Lemonidou, A.A., Vasalos, I.A., 2009. Hydrogen production via reforming of the aqueous phase of bio-oil over Ni/Olivine catalysts in a spouted bed reactor. Ind. Eng. Chem. Res. 48, 1400–1408.

Kechagiopoulos, P.N., Voutetakis, S.S., Lemonidou, A.A., Vasalos, I.A., 2006. Hydrogen production via steam reforming of the aqueous phase of bio-oil in a fixed bed reactor. Energy Fuels 20, 2155–2163.

Lea-Langton, A., Md Zin, R., Dupont, V., Twigg, M.V., 2012. Biomass pyrolysis oils for hydrogen production using chemical looping reforming. Int. J. Hydrogen Energy 37, 2037–2043.

Li, H., Xu, Q., Xue, H., Yan, Y., 2009. Catalytic reforming of the aqueous phase derived from fast-pyrolysis of biomass. Renewable Energy 34, 2872–2877.

Li, Q., Steele, P.H., Mitchell, B., Ingram, L.L., Yu, F., 2013. The addition of water to extract maximum levoglucosan from the bio-oil produced via fast pyrolysis of pretreated loblolly pinewood. Bioresour. Com. 8, 1868–1880.

Marquevich, M., Medina, F., Montané, D., 2001. Hydrogen production via steam reforming of sunflower oil over Ni/Al catalysts from hydrotalcite materials. Catal. Commun. 2, 119–124.

McBride, B.J., Gordon, S., 1996. Computer Program for Calculation of Complex Chemical Equilibrium Compositions and Applications II. Users Manual and Program Description. NASA Lewis Research Centre.

Md Zin, R., Lea-Langton, A., Dupont, V., Twigg, M.V., 2012. High hydrogen yield and purity from palm empty fruit bunch and pine pyrolysis oils. Int. J. Hydrogen Energy 37, 10627–10638.

Medrano, J.A., Oliva, M., Ruiz, J., García, L., Arauzo, J., 2011. Hydrogen from aqueous fraction of biomass pyrolysis liquids by catalytic steam reforming in fluidized bed. Energy 36, 2215–2224.

Mosteiro-Romero, M., Vogel, F., Wokaun, A., 2014. Liquefaction of wood in hot compressed water Part 1 – Experimental results. Chem. Eng. Sci. 109, 111–112.

Neveux, N., Yuen, A.K.L., Jazrawi, C., Magnusson, M., Haynes, B.S., Masters, A.F., Montoya, A., Paul, N.A., Maschmeyer, T., de Nys, R., 2014. Bio crude yield and productivity from the hydrothermal liquefaction of marine and freshwater green macroalgae. Bioresour. Technol. 155, 334–341.

Ni, M., Leung, D.Y.C., Leung, M.K.H., 2007. A review on reforming bio-ethanol for hydrogen production. Int. J. Hydrogen Energy 32, 3238–3247.

Pimenidou, P., Rickett, G., Dupont, V., Twigg, M.V., 2010. High purity H_2 by sorption-enhanced chemical looping reforming of waste cooking oil in a packed bed reactor. Bioresour. Technol. 101, 9279–9286.

Saidi, M., Samimi, F., Karimpourfard, D., Nimmanwudipong, T., Gates, B.C., Rahimpour, M.R., 2014. Upgrading of lignin-derived bio-oils by catalytic hydrodeoxygenation. Energy Environ. Sci. 7, 103–129.

Sipila, K., Kuoppala, E., Fagernas, L., Oasmaa, A., 1998. Characterisation of biomass-based flash pyrolysis oils. Biomass Bioenergy 14, 103–113.

Sukhbaatar, B., Li, Q., Wan, C., Yu, F., El-Barbary, H., Steele, P., 2014. Inhibitors removal from bio-oil aqueous fraction for increased ethanol production. Bioresour. Technol. 161, 379–384.

Yan, C.-F., Cheng, F.-F., Hu, R.-R., 2010. Hydrogen production from catalytic steam reforming of bio-oil aqueous fraction over Ni/CeO$_2$–ZrO$_2$ catalysts. Int. J. Hydrogen Energy 35, 11693–11699.

Yaws, C.L., 2009. Yaws' Handbook of Thermodynamic Properties for Hydrocarbons and Chemicals. Knovel.

Ye, L., Zhang, J., Zhao, J., Tu, S., 2014. Liquefaction of bamboo shoot shell for the production of polyols. Bioresour. Technol. 153, 147–153.